(13) Nieduszynski, I. A.; Marchessault, R. H. *Biopolymers* **1972**, *11*, 1335.
(14) Shepherd, L.; Chen, T. K.; Harwood, H. J. *Polym. Bull.* **1979**, *1*, 445,
(15) Natta, G.; Corradini, P. *Makromol. Chem.* **1955**, *16*, 77.
(16) Atkins, E. D. T.; Keller, A.; Shapiro, J. S.; Lemstra, P. J. *Polymer* **1981**, *22*, 1161.
(17) Alexander, L. E. "X-ray Diffraction in Polymer Science"; Wiley-Interscience: New York, 1969; p 189.
(18) Keith, H. D. *J. Polym. Sci., Part A* **1964**, *2*, 4339.
(19) Guenet, J. M.; Picot, C.; Benoit, H. *Macromolecules* **1979**, *12*, 86.
(20) Reiss, C.; Benoit, H. *C. R. Hebd. Seances Acad. Sci.* **1961**, *256*, 268.
(21) Liu, K.-J.; Ullman, R. *Polymer* **1965**, *6*, 100.
(22) Inoue, Y.; Konno, T. *Polym. J.* **1976**, *8*, 457.
(23) Overbergh, N.; Berghmans, H.; Smets, G. *Polymer* **1975**, *16*, 703. *Ibid.* **1978**, *19*, 602.
(24) Faulkner, D. L.; Hopfenberg, H. B.; Stannett, V. T. *Polymer* **1977**, *18*, 1130.

Crystal Structure of Pristine and Iodine-Doped *cis*-Polyacetylene

James C. W. Chien* and Frank E. Karasz*

Department of Polymer Science and Engineering, Department of Chemistry, Materials Research Laboratory, University of Massachusetts, Amherst, Massachusetts 01003

Kaoru Shimamura

Institute for Chemical Research, Kyoto University, Uji 611, Japan.
Received November 4, 1981

ABSTRACT: Acetylene has been polymerized directly onto the electron microscope grid at −78 °C to produce ultrathin films of *cis*-$(CH)_x$ having regions of oriented fibrils. An electron beam directed at these fibrils gave fiber electron diffraction patterns. Pristine *cis*-$(CH)_x$ has an orthorhombic unit cell with $a = 7.68$, $b = 4.46$, and $c = 4.38$ Å. The fiber and molecular axes are along c. The space group is *Pnam*, with a setting angle of 31–33° for the cis-transoid structure and 34–36° for the trans-cisoid structure. The structure contains nonbonded interactions between some of the atoms in the unit cell. *cis*-$(CH)_x$ doped by iodine to the semiconducting state showed all the unperturbed reflections of undoped *cis*-$(CH)_x$. In addition, there are present meridional reflections of undoped *trans*-$(CH)_x$ and new ones arising from the doped structure. Heavily iodine-doped metallic polyacetylene had electron diffraction entirely different from that of the undoped polymers. A structure is proposed for this material.

Introduction

Acetylene can be polymerized as predominantly *cis*-$(CH)_x$ or *trans*-$(CH)_x$ under proper conditions,[1-3] the latter being the thermodynamically more stable isomer. In fact, *cis*-$(CH)_x$ can be readily isomerized to *trans*-$(CH)_x$ by heating in vacuo.[2-5] Pristine *cis*-$(CH)_x$ is free of unpaired spins[6] when polymerized at −78 °C. Upon warming up to room temperature, there is some isomerization,[4] producing about one neutral soliton per 25 000 CH units. The polymer is flexible and can be stretched about threefold. *cis*-$(CH)_x$ has a room-temperature conductivity[7] of ca. 10^{-9} $(\Omega\ cm)^{-1}$. By comparison, *trans*-$(CH)_x$ is brittle, contains one soliton per 1000–3000 CH units, and has a room-temperature conductivity of 10^{-5} $(\Omega\ cm)^{-1}$. Knowledge of their structures is essential to the understanding of the properties of polyacetylene.

We have developed a method to prepare very thin films (~1000 Å) directly on the electron microscope grid.[8] By repeated washing of the polymer and evaporation of solvent, there were formed regions of oriented bundles of polyacetylene fibrils. Analysis of the electron diffraction from these oriented fibrils yielded the crystal structure of *trans*-$(CH)_x$.[9]

The crystal structure of undoped *cis*-$(CH)_x$ was first studied by Baughman et al. with X-ray diffraction[10] on randomly oriented specimens. Ten reflections were observed; seven of them are very broad. Together with packing calculations, Baughman et al. concluded that the unit cell is orthorhombic, containing two molecules and a *Pnam* space group. Lieser et al.[11] reported electron diffraction results on *cis*-$(CH)_x$. Only equatorial reflections were observed at normal electron beam incidence. Upon tilting of the specimen, the (001) and (221) reflections become observable. The two studies agreed in the unit cell dimensions. They differ in the indexing of reflections. Lieser et al.[11] stated that their samples have a space group different from *Pnam*, a folded-chain morphology, and the c axis (molecular axis) perpendicular to the axis linking the lamellae ("fiber" axis). Baughman et al. assigned the b axis to be the molecular chain axis.

Because of the above-mentioned discrepancies in the *cis*-$(CH)_x$ structure, we have now carried out electron diffraction studies on oriented fibrils of this polymer. The results are in agreement with the X-ray work, except that the c axis has been identified unambiguously *to be the molecular axis and the fiber axis as well.* Therefore, the previous b- and c-axis assignments by Baughman et al.[10] should be interchanged.

In addition, *cis*-$(CH)_x$ has been doped to both the semiconducting state and the metallic state with iodine. Structures for these materials are also described.

Experimental Section

The procedure for in situ acetylene polymerization has been described previously.[8,9] The semiconducting polymer (A) was obtained by doping with I_2; both the specimen and the iodine were maintained at −23 °C ($p_{I_2} = 3 \times 10^{-3}$ mm) for 4 h. *cis*-$(CH)_x$ was heavily doped with iodine to the metallic conducting state (B) by keeping the polymer and iodine at 10 °C overnight ($p_{I_2} = 8.08 \times 10^{-2}$ mm).

A JEOL 100CX EM diffractometer was used in this investigation. The sample was first examined in the transmission mode. Electron diffraction patterns of selected regions of the oriented

0024-9297/82/2215-1012$01.25/0

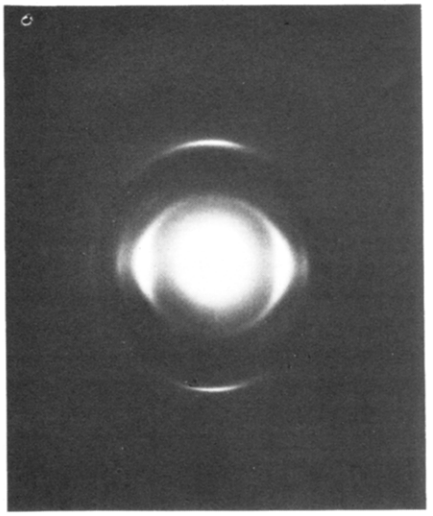

Figure 1. Electron diffraction pattern of pristine *cis*-$(CH)_x$.

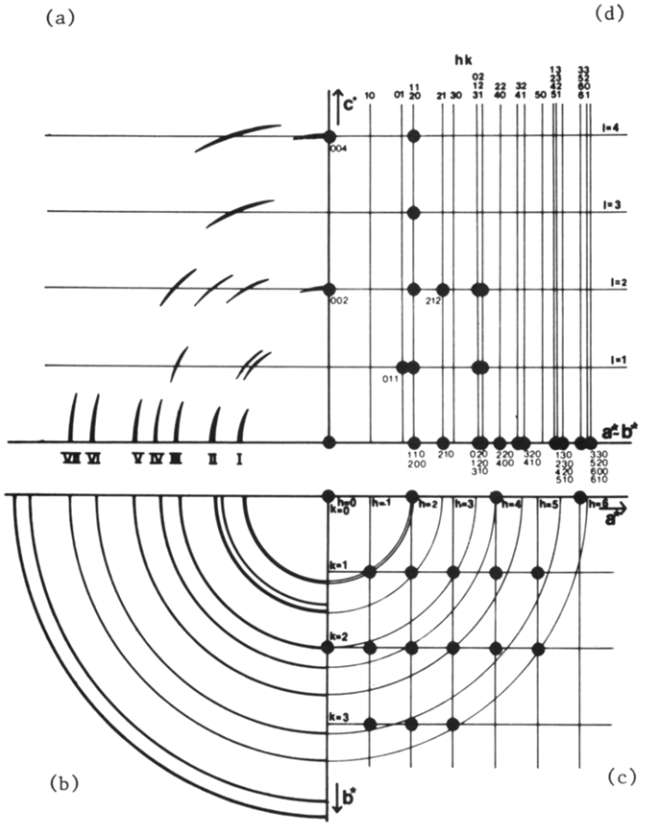

Figure 2. (a) Schematic representation of the electron diffraction of oriented *cis*-$(CH)_x$ fibrils. (b) Schematic representation of the electron diffraction pattern of randomly packed regions. (c) Reciprocal lattice for the a^*b^* plane ((●) observed reflection). (d) Projection of the reciprocal lattice of the first five layer a^*b^* planes.

fibrils were then obtained. Evaporated gold and aluminum were used as reference materials for *d*-spacing calibration. A Nonius microphotometer was used to read photographic intensities of the diffraction lines, and these were converted to diffraction intensities by a calibration curve obtained as a function of exposure.

Results and Discussion

Pristine *cis*-$(CH)_x$. *cis*-$(CH)_x$ has the same fibrillar morphology as *trans*-$(CH)_x$. Typical electron microscopy photographs have been published previously.[8,9] The electron diffraction pattern for aligned fibrils of *cis*-$(CH)_x$ is shown in Figure 1. It is evident that this pattern has

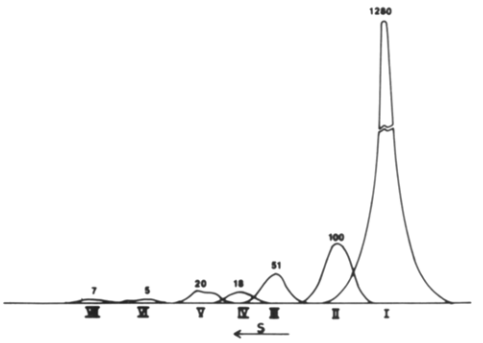

Figure 3. Photographic intensities of the equatorial reflections in Figure 1.

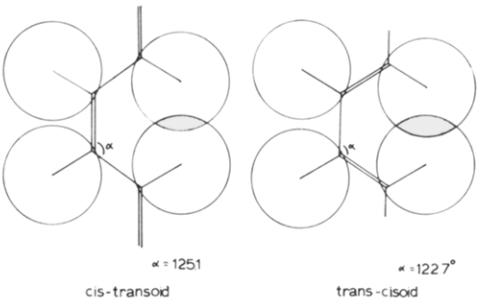

Figure 4. Atomic parameters used to calculate reflection intensities.

more reflections than that for pristine *trans*-$(CH)_x$.[9] Figure 2a is the schematic representation of the electron diffraction of oriented fibrils. Figure 2b is the schematic representation of the Debye rings observed for the randomly packed region of the specimen by electron diffraction. There are observed (002) and (004) meridional reflections for *cis*-$(CH)_x$ whereas only the (002) reflection was seen in the case of *trans*-$(CH)_x$.[9] Also, there are seven equatorial reflections for the former as compared to six in the latter.

The unit cell for *cis*-$(CH)_x$ was arrived at by the following considerations. The four meridional reflections are quite sharp. This indicates strong periodicity along the fiber axis, as polymer molecules generally maintain strong periodicity in their chain axis. So it is concluded that the molecular chain axis is along the fiber axis as in the case of *trans*-$(CH)_x$. This information is obtainable from electron diffraction of partially aligned fibrils but not with randomly packed samples.[10,11]

Extinction of (00*l*) reflections with l = odd requires that the polymer chain have a 2_1 screw axis in the unit cell. The reciprocal lattice is shown in Figure 2c. In Figure 2d, it is seen that *all* the observed reflections fall on the reciprocal lattice site; they have been indexed in Table I. For comparison, the indexing of the X-ray and electron diffraction data by Baughman et al.[10] and Lieser et al.,[11] respectively, are also included in the table.

The unit cell is orthorhombic, with parameters summarized in Table II. The space group is probably *Pnam*, though not with certainty. The reflections for this space group are given in Table III, both for those predicted and observed and for others not found. The observed intensities of the equatorial reflections are shown in Figure 3, the first one, (110) + (200), being much more intense than all the others.

The theoretical reflection intensities were calculated for both the cis-transoid and trans-cisoid structures with the following parameters: C=C = 1.35 Å, C—C = 1.46 Å, C—H = 1.09 Å, and repeat length 4.38 Å, as shown in Figure 4. The structure factors of the (*hk*0) reflections

Table I
Indices for Reflections of Pristine *cis*-$(CH)_x$

this study ED			Baughman et al. X-ray		Lieser et al. ED	
(*hkl*)	d_{obsd}, Å	d_{calcd}, Å	*d*, Å	(*hlk*)[a]	*d*, Å	(*hkl*)
					4.47	(001)
(200)	3.84	3.84			3.85	(200)
(110)		3.86	3.80	(110)	3.78	(110)
(011)	3.06	3.13	3.13	(011)		
(201)	2.92	2.89				
(210)	2.89	2.91	2.87	(210)	2.89	(210)
			2.41	(211)		
(020)						
(120)	2.23	2.23			2.21	(310)
(310)		2.14				
		2.22				
(002)	2.19	2.19	2.19	(020)	2.16	(020)
			2.11	(120)	2.08	(120)
(220)	1.98	1.93	2.00	(311)		
(400)		1.93				
			1.90	(220)	1.89	(220)
(320)	1.70	1.68	1.74	(410)	1.77	(410)
(410)		1.76				
			1.65	(411)	1.66	(320)
(130), (230)	1.42	1.46, 1.39				
(420), (510)		1.46, 1.45				
(330), (520)	1.28	1.29, 1.26			1.26	(520)
(600), (610)		1.28, 1.23				
(004)	1.12	1.10				

[a] (*hlk*) instead of (*hkl*) because Baughman's model takes the *b* axis as the chain axis.

Table II
Unit Cell Parameters for *cis*-Polyacetylene

	present work	Baughman et al.	Lieser et al.
a, Å	7.68[a]	7.61	7.74
b, Å	4.46	4.47[b]	4.32
c, Å	4.38[c]	4.39	4.47
ρ, g cm^{-3}	1.15	1.16	1.16

[a] Estimated error is ±0.02 Å. [b] Baughman et al. assigned *b* to be along the molecular chain axis. [c] Molecular chain axis and fiber axis.

Table III
Reflections for *cis*-Polyacetylene

	reflections		
	present	absent	
hkl	(111), (112), (113), (114), (121), (122), (212), (311)..., all		*P*
0*kl*	(011), (022)?, $k + l$ = even	(012), (021)?, $k + l$ = odd	*n* (⊥*a*)
*h*0*l*	(201), (202), (203), h = even	(101), (102), (301), (302), h = odd	*a* (⊥*b*)
*hk*0	(110), (120), (210), (220), (310), (420), (510)..., all		*m* (⊥*c*) or 1
*h*00	(200), (400)	(100), (300)	
0*k*0	(020), (040)	(010), (030)	
00*l*	(002), (004)	(001), (003)	

were calculated as a function of setting angle ϕ. In cases of overlapping reflections, their calculated intensities are summed. Figure 5 shows the calculated intensities vs. ϕ for the trans-cisoid structure.

The reliability factor is defined as

$$R = \sum(||F_{obsd}| - |F_{calcd}||)/\sum|F_{obsd}| \quad (1)$$

where F_{obsd} is proportional to $(I_{obsd} \sin(2\theta))^{1/2}$, where I is the intensity. In Figure 6, plots of R vs. ϕ are shown for

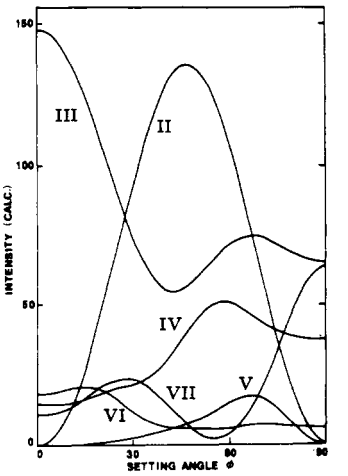

Figure 5. Calculated reflection intensities as a function of ϕ for *cis*-$(CH)_x$. Because of the much stronger observed and calculated intensities of reflection I over those of reflections II–VII, relative intensities among reflections II–VII are shown here.

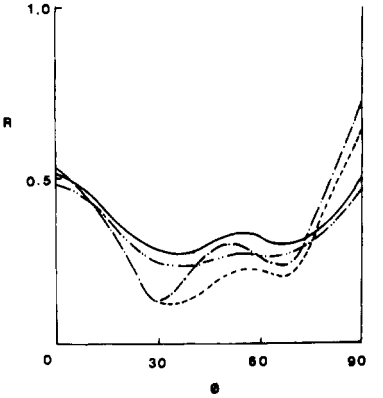

Figure 6. Variation of the reliability factor with setting angle ϕ: (—) cis transoid for reflections I–VII; (-·-) cis transoid for reflections II–VII; (-··) trans cisoid for reflections I–VII; (---) trans cisoid for reflections II–VII.

Table IV
Observed and Calculated Electron Diffraction Intensities for Pristine cis-(CH)$_x$

reflection	spacing, Å	e, m, or off[a]	width[b]	(hkl)	intensity obsd[c]	intensity cis transoid $\phi = 32°$	intensity trans cisoid $\phi = 32°$
I	3.84	e	B	110	963 vs	727	829
				220			
	3.06	off		011	m		
	2.92	off	N	201	m		
II	2.89	e	N	210	100 s	100	100
III	2.23	e	B	020	66 s	59	68
				120			
				310			
	2.19	m	N	002	vs		
IV	1.98	e	B	220	26 m	20	22
				400			
V	1.70	e	B	320	34 m	3	4
				410			
VI	1.42	e	vB	130, 230, 420, 510	10 vw	8	8
VII	1.28	e	vB	330, 520, 600, 610	16 w	22	23
	1.10	m	N	004	m		

[a] e = equatorial, m = meridional, off = off meridional. [b] B = broad, N = narrow, vB = very broad. [c] I_{obsd} sin (2θ); vs = very strong, s = strong, m = medium, w = weak, vs = very weak.

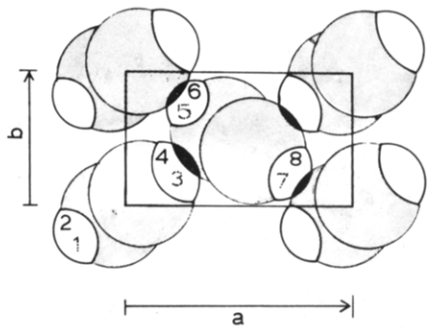

Figure 7. Molecular conformation of *cis*-(CH)$_x$.

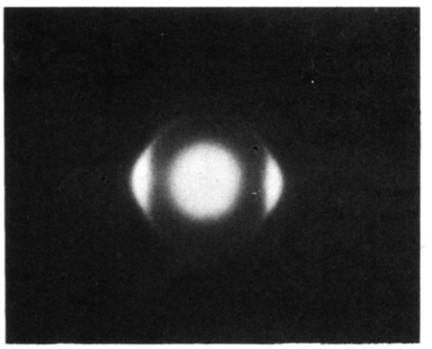

Figure 8. Electron diffraction pattern of aligned fibrils in sample A (*cis*-(CH)$_x$ doped with iodine to the semiconducting state).

both the cis-transoid and the trans-cisoid structures. In addition, the reliability factors were calculated in one case including all seven equatorial reflections and in another using only reflections II–VII. The latter was done to reduce the overwhelming contribution of the first equatorial reflection, which has a very high intensity (Figure 3). The curves in Figure 6 showed that by excluding reflection I, the minima in R are sharper and the setting angles are slightly different from the results using all equatorial reflections. The best setting angle is 31–33° for cis transoid and 34–36° for trans cisoid. Table IV compares the observed and calculated intensities of the cis-transoid and trans-cisoid ($hk0$) reflections.

Figure 7 shows the molecular conformation of *cis*-(CH)$_x$ in the crystal. The black regions in the figure correspond to CH separations of only 2.70 Å, which is less than their van der Waals radii of 1.80 + 1.17 Å = 2.97 Å. This may be the reason why *cis*-(CH)$_x$ is so unstable and facile isomerization occurs even below room temperature. However, this nonbonded interaction may not be real and can be eliminated by refinement in calculation such as including a slight twisting of a few degrees of the *cis*-(CH)$_x$ backbone. Measurements are under way to obtain electron diffraction of greater precision, and refinement in calculations are being made. In comparison, there are no packing conflicts in the crystal structure of *trans*-(CH)$_x$.[9] Furthermore, the adjacent monomer units along the b axis are parallel in *trans*-(CH)$_x$, and π-orbital overlaps between them are possible. This is not the case in *cis*-(CH)$_x$, which may contribute toward the differences in their conductivities.

***cis*-(CH)$_x$ Doped with Iodine to the Semiconducting State.** *cis*-(CH)$_x$ was doped with iodine at −23 °C for 4 h. The sample was kept at −78 °C for a short while before it was transferred into the electron microscope with a cold stage maintained at −150 °C. Transmission EM photographs show beadlike morphology. Several interpretations are possible: (a) there are deposits of I_2 microcrystals, (b) there are aggregates of iodine-doped region, (c) there are spiral overgrowths on the fibrils, and (d) iodine acts as decoration helping to render noticeable the overgrowth. In this particular case, the beads disappeared upon warming of the sample to room temperature, suggesting (a) or (b) as the possible explanation. Nevertheless, such observations made us curious and led to an intense investigation and the finding of polymorphism in undoped (CH)$_x$, which will be published elsewhere.

Careful comparison with EM photographs of undoped polyacetylene[9] showed that neighboring fibrils may have been fused together by doping.

The electron diffraction pattern of the aligned fibrils in sample A is shown in Figure 8, and Figure 9 is a schematic representation of it. The pattern is more complicated than that of undoped *cis*-(CH)$_x$. All the equatorial reflections can be assigned to the pristine *cis*-(CH)$_x$. Therefore, most of the *cis*-(CH)$_x$ retains its crystal structure; the mole fraction of iodine in the sample is between 10^{-3} and 10^{-2}. Along the meridian there are reflections corresponding to (002) and (004) of *cis*-(CH)$_x$. However, there are also reflections assignable to (002) of *trans*-(CH)$_x$. In addition, there are new reflections that do not correspond to any

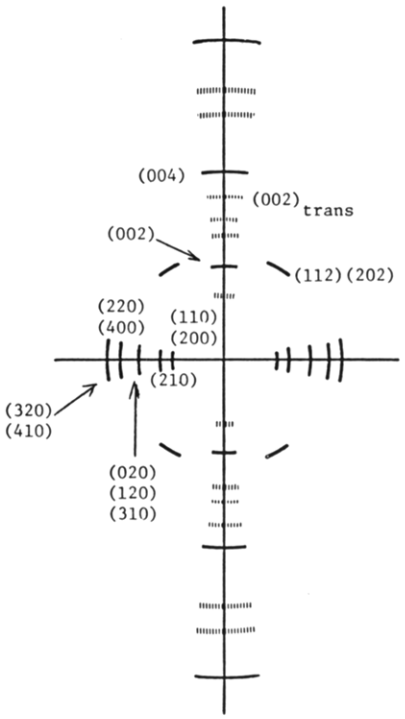

Figure 9. Schematic representation of the electron diffraction pattern in Figure 8.

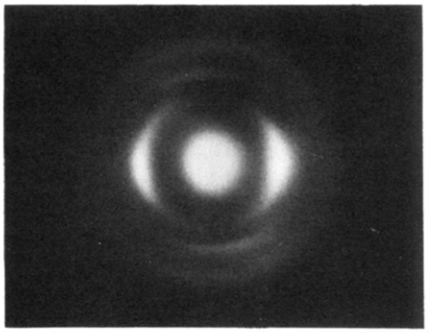

Figure 10. Electron diffraction pattern of aligned fibrils in sample B (*cis*-$(CH)_x$ saturation doped with iodine to the metallic state).

Table V
Observed and Reciprocal Spacings s_i for the Meridional Reflections in Polyacetylene Saturation Doped with Iodine

intensity peak, i	$s_i = (\sin\theta_i)/\lambda$[a]	s_i/s_1 obsd	s_i/s_1 calcd for I–I = 3.3 Å
1	0.16 (=s_1)	1.0 vs	1.0
2	0.26	1.63	1.54
3	0.32	1.98 m	2.03
4	0.37	2.27	
5	0.41	2.50 s	2.51
			2.86
6	0.53	3.28	3.17
7	0.63	3.88	3.63
8	0.69	4.29	4.11

[a] s_i corresponds to the distance of the ith peak from the center of the electron diffraction pattern.

spacings of either of the undoped polyacetylene structures. These are apparently the reflections from the new doped structure.

The above results suggest that doping can promote isomerization of polyacetylene even at low temperatures.

***cis*-$(CH)_x$ Doped with Iodine to the Metallic State.** This sample exhibits very broad equatorial reflections and

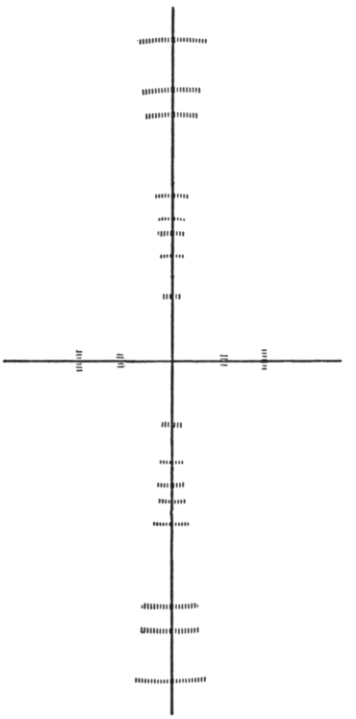

Figure 11. Schematic representation of diffraction in Figure 10.

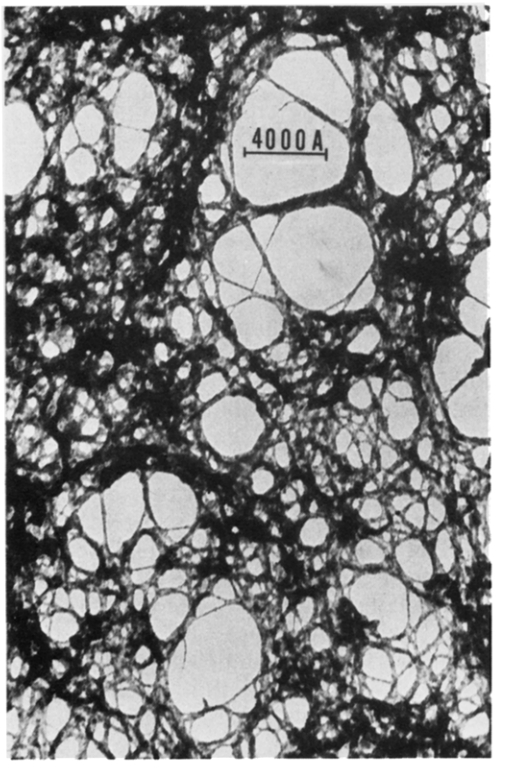

Figure 12. Electron microscopy photograph of sample B.

eight broad meridional reflections (Figures 10 and 11). The transmission EM photograph (Figure 12) showed the polymer retains fibrillar morphology. The fibrils appear to have fused together and/or swollen, and some regions seem to contain more dopants than others. Very dark regions are probably a thick mat of randomly packed polyacetylene fibers.

None of the reflections can be attributed to the *cis*-$(CH)_x$ spacings. Attempts to index these reflections have been made but no reasonable sets of indices were found. The intensity distribution is believed to be mainly due to the structure factor; i.e., intensity corresponds to scattering

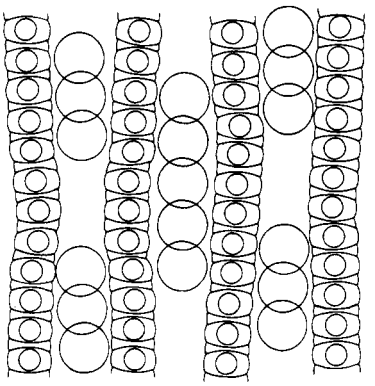

Figure 13. Packing arrangement for polyacetylene doped with iodine to the metallic state.

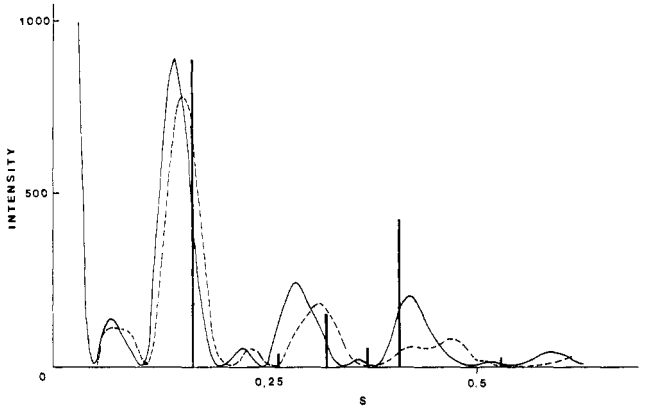

Figure 14. Observed and calculated intensity distribution for meridional reflections in polyacetylene saturation doped with iodine. Heights of bold bars show observed relative intensities. The peaks are so broad that experimental error of the peak positions is ca. ±0.02 Å^{-1}. Calculated intensity distributions are shown by thin lines: (– – –) for I–I bond length in I^{x-} (3.3 Å); (—) for I–I bond length in I_x^- (3.5 Å).

from independent sets of polyacetylene chains and I_x, without correlation between the sets.

A model for saturation-doped polyacetylene is proposed here based on the following considerations. Two Raman bands in iodine-doped polyacetylene have been assigned[13] to I_3^- and I_5^-. The variation of soliton concentration with iodine doping[5,14] also supports this assignment. At saturation doping, the polyacetylene contains about 10–20 mol % iodine atoms. Assuming I_3^- to be the main dopant species, there is about one I_3^- per 14–28 CH units. Taking the length of I_3^- to be 10.2 Å and the diameter of the iodine atom to be 3.96 Å, we propose the model in Figure 13. Therefore, not all CH units have neighboring dopant. In these vacancy regions the interchain distance is smaller than in those regions with dopants. This causes broadening of the equatorial reflections and only a few reflections are observable.

Implicit in this model is that the π orbitals perpendicular to the polyacetylene chains interact with the iodine. Atomic distances of I and C suggest that the interchain distance is $3.96 + 3.6 \approx 7.6$ Å, which is about twice the observed spacing of 3.8 Å. Another observed reflection corresponds to the interplane distance of 2.19 Å. Calculations have been carried out for reflection intensities along the meridian. The results are shown in Figure 14. The relative spacings for these reflections are summarized in Table V for both experimental and calculated values.

The agreement of the model-predicted reflection spacings and intensities with observation is fairly good for the smaller iodine–iodine distances. The model appears reasonably good and more measurements are under way to refine the model further.

Acknowledgment. This work was supported by a National Science Foundation grant.

References and Notes

(1) Ito, T.; Shirakawa, H.; Ikeda, S. *J. Polym. Sci., Polym. Chem. Ed.* **1974**, *12*, 11.
(2) Shirakawa, H.; Ikeda, S. *Polym. J.* **1971**, *2*, 231.
(3) Ito, T.; Shirakawa, H.; Ikeda, S. *J. Polym. Sci., Polym. Chem. Ed.* **1975**, *13*, 943.
(4) Chien, J. C. W.; Karasz, F. E.; Wnek, G. E. *Nature (London)* **1980**, *285*, 390.
(5) Chien, J. C. W. *J. Polym. Sci., Polym. Lett. Ed.* **1981**, *19*, 249.
(6) Chien, J. C. W.; Karasz, F. E.; Wnek, G. E.; MacDiarmid, A. G.; Heeger, A. J. *J. Polym. Sci., Polym. Lett. Ed.* **1980**, *18*, 45.
(7) MacDiarmid, A. G.; Heeger, A. J. *Synth. Met.* **1979/1980**, *1*, 101.
(8) Karasz, F. E.; Chien, J. C. W.; Galkieincz, R.; Wnek, G. E.; Heeger, A. J.; MacDiarmid, A. G. *Nature (London)* **1979**, *282*, 286.
(9) Shimamura, K.; Karasz, F. E.; Hirsch, J. A.; Chien, J. C. W. *Makromol. Chem., Rapid Commun.* **1981**, *2*, 473.
(10) Baughman, R. H.; Hsu, S. L.; Pez, G. P.; Signorelli, A. J. *J. Chem. Phys.* **1978**, *68*, 5405.
(11) Lieser, G.; Wegner, G.; Muller, W.; Enkelmann, V. *Makromol. Chem., Rapid Commun.* **1980**, *1*, 621.
(12) TraeHeberg, M. *Acta Chem. Scand.* **1968**, *22*, 628, 2294.
(13) Hsu, S. L.; Signorelli, A. J.; Pez, G. P.; Baughman, R. H. *J. Chem. Phys.* **1978**, *69*, 1.
(14) Chien, J. C. W.; Wnek, G. E.; Karasz, F. E.; Warakomski, J.; Dickinson, L. C.; MacDiarmid, A. G.; Heeger, A. J. *Macromolecules* **1982**, *15*, 614.